Available online at www.sciencedirect.com

Manufacturing Letters

Manufacturing Letters 00 (2023) 000–000

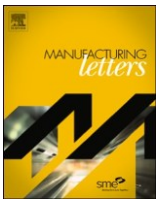

51st SME North American Manufacturing Research Conference (NAMRC 51, 2023)

Template-free scalable roll-to-roll fabrication of textured transparent film for passive radiation cooling of photovoltaics

Myers Harbinson[a,1], Michael Pudlo[a,1], Sipan Liu[a,1], Taimur Chaudhry[a], Yuxuan Liu[a], Chenxi Sui[b], Yong Zhu[a], Po-Chun Hsu[b], Jong E. Ryu[a,*]

[a]*Department of Mechanical and Aerospace Engineering, NC State University, Raleigh, NC, USA*
[b]*Pritzker School of Molecular Engineering, University of Chicago, Chicago, IL, USA*

Abstract

Solar panels contributed to over 115,000 GWh of energy being produced in the United States and solar panel energy consumption has increased by 27 % at the start of the 21st century. Given the decrease of photovoltaic efficiency at higher temperatures and the increasing demand for clean energy, the development of an economical technology for solar panel cooling is necessary. Passive cooling can be achieved by infrared radiating into space. Typical solar arrays require large functional areas in order to supply a significant amount of power as compared to other sources. As such, any method to help reduce the temperature of the solar panel surfaces needs to maintain manufacturing scalability for sustainable use. We demonstrate a rapid, low-cost, template-free roll coating method to fabricate photonic composite film with SiO_2 nanoparticles which possess high emissivity in the atmospheric transparent window while passing visible and near infrared light to photovoltaics beneath. When facing direct sunlight at summer noon, the coatings show a 3.5°C temperature decrease without loss of photovoltaic efficiency while having hydrophobic and contamination-resistance merits.

Keywords: Roll Coating; Scalable Manufacturing; Passive Cooling; Photovoltaics; Micro-structures; Nanoparticles

1. Introduction

With the global temperature on the rise, renewable energy has become increasingly popular. Solar energy consumption saw a 27% increase per year at the start of the 21st century largely due to increasing solar panel installation in residential applications [1]. In 2020, solar photovoltaic energy accounted for over 115,000 GWh of energy being produced in the United States, with significant additions around the world as well [2]. With this increase in solar energy, it is essential that solar panels function at the highest possible efficiency. Both dust and increased temperatures are detrimental to the efficiency of photovoltaic panels. As such, it is necessary to develop mitigation for these hazards.

Most silicon-based photovoltaic cells generate power using visible light and part of the near-infrared (IR) (0.4 - 1.1 μm) [3]. All other wavelengths are absorbed by the panel as heat. Electrical losses also contribute to the heating of solar cells. Solar panel efficiency, is inversely proportional to the temperature of the photovoltaic cell. It is known that a 1°C increase in temperature can lower the efficiency of a solar cell by 0.4-0.5% [4, 5]. Furthermore, prolonged exposure to increased temperature can decrease the lifespan of photovoltaic panels [3, 6]. Therefore, maintaining a low operational temperature is essential to optimize the function of solar cells.

*Corresponding author. Tel.: +1-919-515-5265
E-mail address: jryu@ncsu.edu (Jong E. Ryu).

[1]These authors contributed equally to this work

Most previous methods of cooling photovoltaics involve increasing the convective heat transfer between the solar cell and the surrounding air. This has been demonstrated using both water and air as heat transport mechanisms [5]. These methods act by transferring heat from the solar cell to a transport medium and dissipating excess via a heat exchanger [5]. While these methods were proven to be effective, they require additional hardware to be added to the solar cell making them more expensive, bulky, and less efficient for industrial applications.

To mitigate the need for extra hardware, recent research has shifted to the use of passive radiative cooling films. These films cool the underlying surface by reflecting much of the incoming light as well as promoting increased mid-infrared emission which is radiated back into space through the atmospheric transparent window (8-13 μm) [7, 8, 9].

Recent studies have shown that passive cooling using nanoparticle composites and photonic structures could be an effective method for cooling solar panels [3, 5, 10, 11, 12, 13]. Cui et. al. demonstrated that transparent passive cooling films capable of cooling the underlying surface by up to 14.95°C could be created by dispersing ZnO nanoparticles in a low-density polyethelene matrix [7]. Lei et. al. developed a nanocomposite film using SiO_2 particles embedded in a polymethyl methacrylate matrix that could cool the underlying surface 4-5°C below ambient temperature using a compression molding process [25]. Precise process control is required in to apply appropriate amounts of pressure to avoid substrate damage. Precise molding temperature, molding pressure, and holding time are critical variables in the compression molding process, which can impact polymer performance [14]. Linshaung et. al. fabricated a transparent radiative cooling layer composed of SiO_2 gratings on an Si wafer simulating the Si-based photovoltaics using the UV photolithography process [13]. Both photolithography and compression molding are time and material intensive. Furthermore, these manufacturing methods tend to be costly and are not scalable. New manufacturing methods must be developed to meet the increased demand for solar energy.

In this research, novel manufacturing methods for the creation of photonic passive cooling surfaces using a roll coating process, which has manufacturing advantages in terms of cost as well as scalability are developed. In this process, as viscous material passes through the gap between two rollers, a positive pressure gradient is made in the coating meniscus downstream [15]. The pressure gradient, along with shearing stress applied by the coating roller, causes instabilities and defects to form [16, 17]. This instability, when a certain critical value is reached, causes linear patterns, ribboning, or spiked defects to appear on the surface [18, 19]. The key manufacturing parameters which influences what type of surface is generated is the roller gap, which influences the pressure gradient, and the roller speed, which influences the shear rate. High shear rates coupled with a small roller gap will create higher density randomly spiked patterns. This manufacturing process is shown in Fig. 1. Similar interfacial behavior is often observed in the texture of walls painted by the roll-brush. Typically, these defects disappear after being extruded through the roller gap because the material's surface tension causes the defects to flatten over time. This property of viscous materials can be manipulated by adding nanoparticles to modify the materials rheological properties. The addition of nanoparticles can also carry secondary

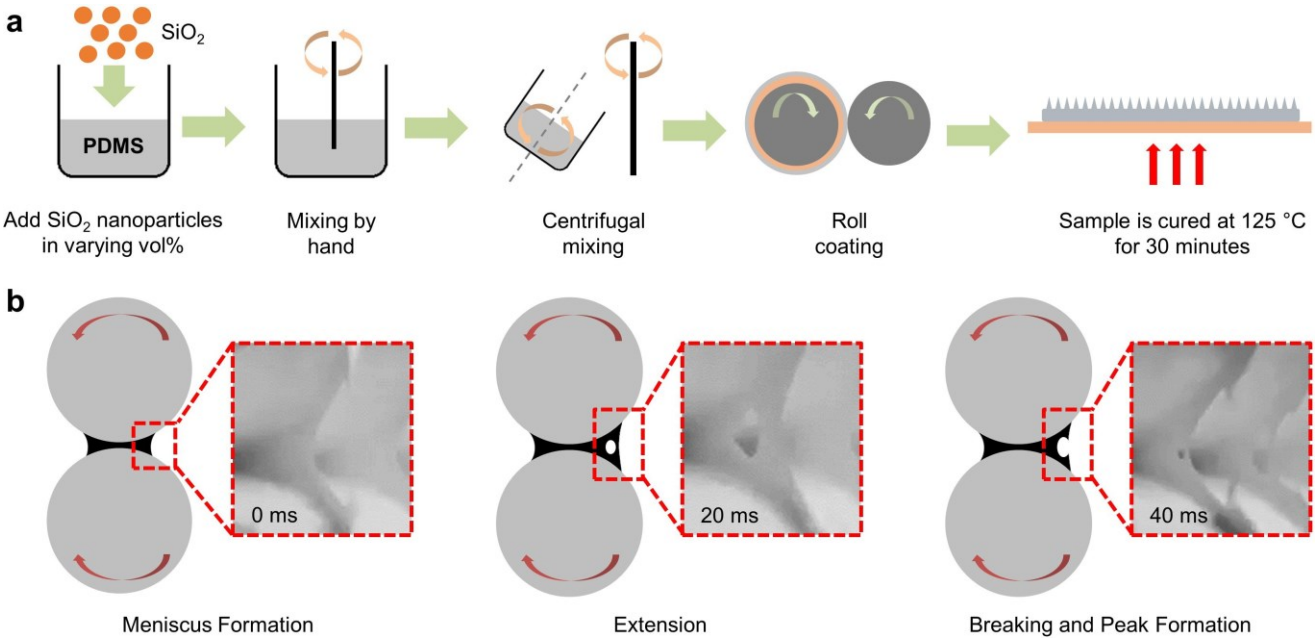

Fig. 1. (a) Manufacturing process for creating SiO_2/PDMS films. Nanoparticles are added in varying volume percentages and then mixed both by hand and using centrifugal mixing. The mixture is then roll coated. Different surface textures are created by varying roller distance and speed. Samples are cured for 30 minutes at 125 °C. (b) Process of forming the surface texture using roll coating. A meniscus is formed due to pressure gradients in the fluid. This meniscus is then stretched and broken to form peaks and ridges. This process occurs continuously along the roller and occurs in about 40 ms.

effects such as increasing the materials IR emittance or solar reflectance. With added nanoparticles, the viscosity and yield strength dominate over the surface tension. The size and spacing of the defect peaks were demonstrated to have a correlation with material properties (such as surface energy and viscosity) along with manufacturing parameters (roller radius, roller gap, and roller speed) [20]. By adding varying fractions of nanoparticles and changing manufacturing parameters, the topology of fabricated films can be manipulated to desired constraints.

In this research, SiO_2/Polydimethylsiloxane (PDMS) nanocomposite films were developed using roll coating methods for use in the passive cooling of solar cells. These films were designed to have rough surface textures to promote increased radiation emittance and anti-fouling properties. The composite films were designed with two optical criteria in mind: Visible transparency, and high mid-IR emission. Furthermore, the films were designed to have very rough surface textures in order to promote increased emission as well as create possible anti-fouling properties.

Ultraviolet-Visible (Uv-Vis) and FTIR spectroscopy were performed in order to characterize the optical properties of the material. The surface roughness was characterized by laser confocal microscopy and measurement of the water contact angle (WCA). Images of the water contact angle were measured by a goniometer. The images were then processed using an open source software named ImageJ. Finally, the films performance on solar cells was characterized by outdoor solar panel tests.

2. Methodology

2.1. Materials

To create the films, an appropriate amount of Sylgard 186 silicone elastomer (purchased from Krayden, Inc) was measured. Varying volume percentages of SiO_2 nanoparticles were then added into the mixture. The SiO_2 nanoparticles are spherical in shape with average diameter of 20-30 nm (purchased from US-nano, Inc.). Hardener was added to this mixture in a 10:1 ratio of PDMS/hardener. This mixture was initially stirred by hand. Once a uniform paste had been formed, it was placed in a centrifugal mixer for 10 minutes before being roll coated.

Polydimethylsiloxane was chosen as the substrate due to its high IR emission. Fourier-Transform infrared (FTIR) spectroscopy reveals peaks at 3 μm as well as a series of peaks between 6-20 μm range [21]. SiO_2 nanoparticles were chosen to modify the viscosity of PDMS because they have high IR emission while maintaining visible transparency [8, 22, 23]. SiO_2 particles are able to enhance the mid-IR emission due to the absorption peak at 9 μm [24]. Furthermore, since appropriate transparency in the solar spectrum is a crucial requirement for any solar panel cooling film, SiO_2 nanoparticles were chosen because they closely match the refractive index of PDMS and avoid the nanoparticle scattering (n_{PDMS} = 1.43, $n_{S\ iO_2}$ = 1.45) [25, 26].

2.2. Roll Coating Process

Eight different SiO_2/PDMS films were manufactured for this experiment: Four flat and four rough films with 4, 6, 8 and 10 volume percent of SiO_2 (10, 14, 18, 21 weight percent). The machine used to fabricate the samples had 2 rollers each with radius 25.4 mm and 300 mm in length. The speed, direction, and distance of each roller was able to be individually controlled. One roller was coated in a layer of Kapton tape which allowed the samples to be easily removed from the roller after the roll coating process was complete. Initially, both rollers were kept at rest and the SiO_2/PDMS paste was spread on the rollers. The speed of each roller was then simultaneously increased. All samples tested in this report were fabricated using a roller distance of 0.1 mm and a roller speed of 100 rpm.

To manufacture films with a flat surface, the paste of nanoparticles and PDMS was spread on the rollers. The speed of one roller was then slowly increased to 100 rpm while the other roller was kept stationary. This caused the paste to be spread over the moving roller in an even film. To manufacture the rough films, the PDMS was spread on the rollers as before.

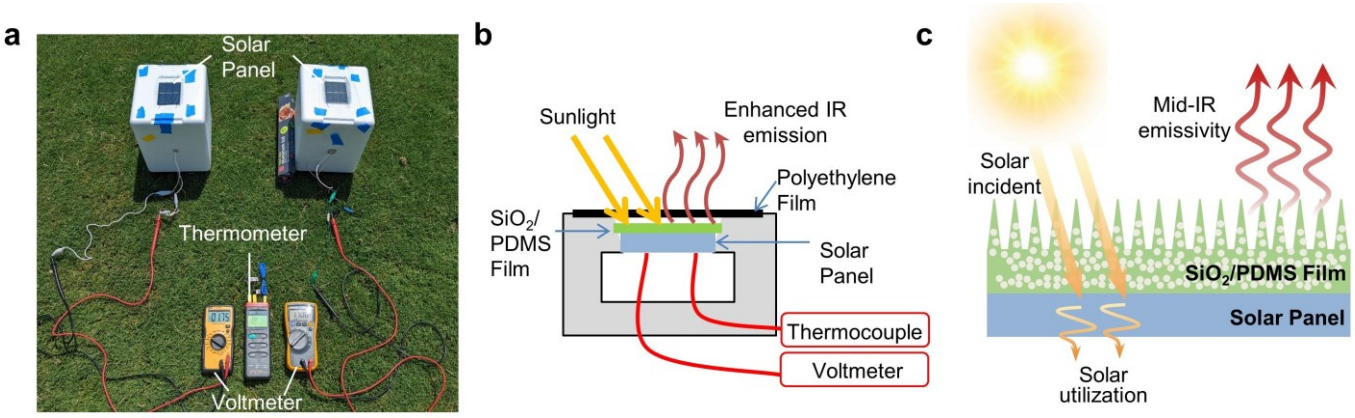

Fig. 2. (a) Solar panel film test procedure. The solar panels are placed in a slot within a styrofoam cooler to insulate it from the environment, along with having a polyethylene film placed overhead to prevent convection. (b) Image of the test setup in use. During the experiment, voltage and temperature are recorded every ten minutes for the span of three hours. (c) The film allows visible light to pass through and be utilized by the solar cell beneath while increasing the Mid-IR emissivity.

Next, the speed of both rollers were simultaneously increased to 100 rpm. After removing the Kapton Tape from the rollers, the films were cured in an oven at 125°C for 30 minutes. This process is shown in Fig. 1 (a).

2.3. Surface Topography Characterization

The surface topography of the rough samples were characterized by a non-contacting laser scanning confocal microscope (Keyence VK-X1100, 0.5 nm height resolution, and 1 nm width resolution). The peak height and density were then evaluated from this data.

The water contact angle of each film was measured by a Rame´-hart goniometer (model 250, with the charge-coupled device camera and a 150 W fiber optic illuminator accessories) at ambient temperature of 23°C. For each sample, 2 μL of water were dropped on the surface. Images were captured at three different locations on each sample. Finally, the water contact angle of each image was found using the drop analysis plugin for ImageJ software.

2.4. Optical Properties Characterization

The reflectance of each film was measured by Uv-Visible spectroscopy spectrometer (UV-Vis, 300–2000 nm, Agilent technologies, Cary 6000i) using a calibrated $BaSO_4$ integrating sphere and a $BaSO_4$ reference at 0.3-1.8 μm. Emittance was measured by a Fourier Transform Infrared spectrometer (FTIR, 4–20 μm, Thermo Scientific, iS50) using a diffuse gold integrating sphere.

2.5. Solar Panel Testing

Outdoor tests were performed in order to test the passive cooling ability of the films as well as evaluate their impact on the power generation of the solar cells. A graphical description of the experimental setup is shown in Fig. 2. A silicon based solar cell was placed in a hole in the lid of a polystyrene container. The purpose of this container was to shield the solar cell from any heat transfer from the environment. The SiO_2/PDMS film was coated on the solar cell by peeling it from the Kapton tape and laying it over the top surface of the solar cell. No additional adhesives were used to secure the film in place. The solar cell and film was then covered with a polyethylene film to ensure that there was no convective heat transfer between the solar panel and the environment. A thermocouple was attached to the back of the solar cell. The voltage output of the solar cell was measured using a voltmeter. Measurements of temperature and voltage were taken every 10 minutes for 3 hours. The outdoor experiments were performed on NCSU's Centennial Campus in Raleigh, North Carolina. Three solar cells were tested at a time. The first solar cell had no film applied to it in order to act as a control sample. The next two cells had the flat and rough SiO_2/PDMS films applied respectively. This allowed for the different volume percents to be compared to a control sample.

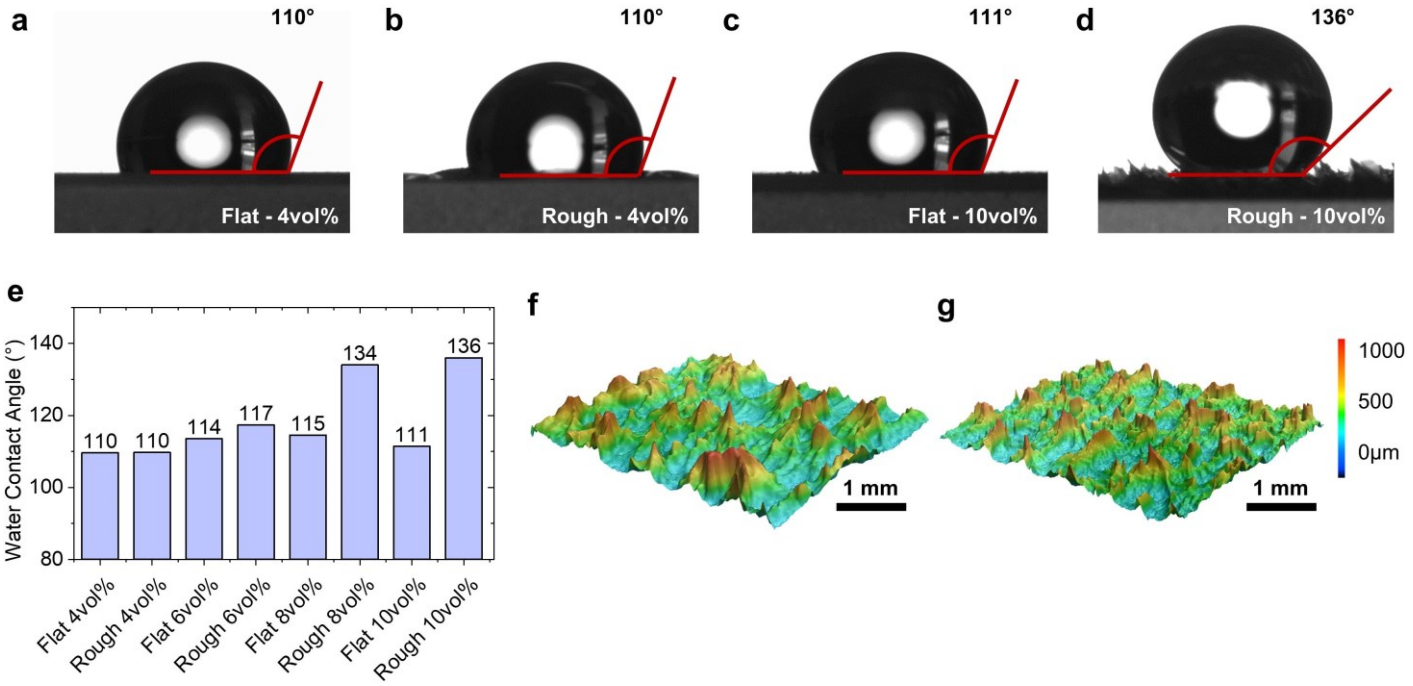

Fig. 3. (a) WCA for the flat 4vol% sample. (b) WCA for the rough 4vol% sample. (c) WCA for the flat 10vol% sample. (d) WCA for the rough 10vol% sample (e) Average water contact angle for each different sample. Surface texture began to have an impact on water contact angle for high volume percents. (f) Laser confocal microscopy of the rough 8 vol% SiO2/PDMS film. Peak spacing is on the order of 400-500 μm with a peak height of 700 μm. (g) Laser confocal microscopy of the 10 vol% SiO2/PDMS film. Peak spacing is on the order of 400-500 μm with a peak height of 600 μm.

3. Results and Discussion

3.1. Surface Characterization

3.1.1. Water Contact Angle

The water contact angle was measured for each sample. The averages are shown in Fig. 3 (a). At low volume percents, there was very little difference between the flat and rough samples. However, for the 8 and 10 percent samples there was an approximately 20° difference in water contact angle between the flat and rough samples. This difference is shown in Fig. 3 (b-e)The difference between high and low volume percent samples is due to the difference in the viscosity of the mixtures. The 4 and 6 volume percent samples were much less viscous than the higher volume percents. As a result, the lower volume percent samples did not hold their shape well and began to flatten as soon as they were removed from the roller.

Surfaces with high water contact angles tend to show anti-fouling merits due to the fact that the surface texture makes it harder for large dust particles to settle on the surface and easier for water to wash away contaminants [27, 28, 29].

The 4 and 6 volume percent samples showed no significant variation in WCA between the flat and rough samples and had poorly defined surface topography in comparison to the 8 and 10 volume percent samples. Due to these poor results, the 4 and 6 volume percent samples were excluded from further experiments.

3.1.2. Laser Confocal

Laser confocal microscopy was performed in order to characterize the surface topology of the 8 and 10 volume percent rough samples and is shown in Fig. 3 (f) and (g). Both the 8 and 10 percent samples have very dense peaks with spacing between 400-500 μm. The peaks on the 8 percent sample are slightly higher than the 10 percent samples. However, the shape of the peaks on the 10 percent film is much sharper. These sharper peaks tend to lead to surfaces with higher water contact angles. Overall, it was seen that the higher volume percent samples were more viscous and led to the formation of sharper less rounded peaks.

3.2. Optical Characterization

Uv-Vis and FTIR Spectroscopy were performed to characterize the optical properties of our coatings. Figure 4 (a) shows the UV-vis spectroscopy for each film. All samples show low absorptance between 400-1100 nm allowing visible light and part of near-IR to be transmitted to the solar cell beneath. The rough samples have higher absorptance than the flat samples of the same volume percent. This shows the ability of the micro structure to increase emittance and shows promise for use in radiative cooling.

Figure 4 (b) shows the FTIR data for each film. All samples have high absorptance with three notable dips at 9.1, 9.8, and 12 μm which matches the atmospheric window (shown in blue). Between the 8 and 10 volume percent samples, the rough samples have higher absorptance than the flat samples and the volume percent of SiO_2 shows no significant impact on absorptance.

3.3. Outdoor Solar Panel Passive Cooling Tests

All outdoor solar panel tests were conducted in Raleigh, North Carolina on NCSU's Centennial Campus (35.77°N - 78.68°E). The solar panel test of the 8 volume percent film was conducted on August 9th, 2022 which featured rare passing clouds. This experiment begun at 10:30 A.M. and lasted 3 hours with humidity ranging from 66% at the start of the test to 60% at the end. Additionally, outdoor air temperature ranged from 30.5°C at the start to 34.4°C at the tests end. The test of the 10 volume percent film was conducted on September 1st, 2022 which featured mostly sunny skies with passing clouds. This experiment began at 3:20 P.M. featuring a 3 hour duration, being conducted later in the day as the morning featured completely cloudy skies. The humidity ranged from 38% at the start of the experiment to 50% at the end. Temperature ranged from

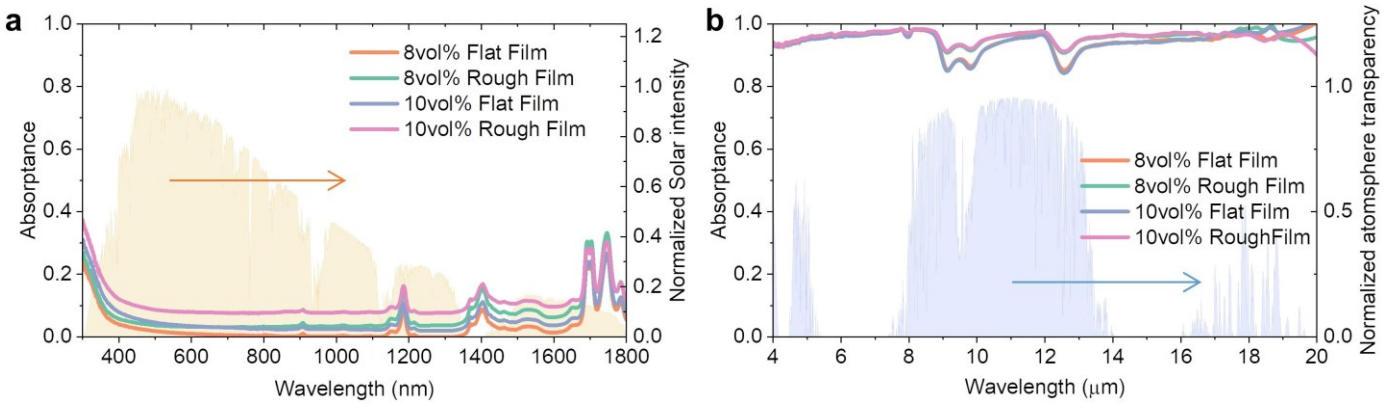

Fig. 4. (a) Uv-Vis spectroscopy of SiO_2/PDMS textured and rough films. All films showed visible transparency with increased absorptance in UV and Near IR wavelengths. The rough films and high volume percent films show the highest absorptance. (b) FTIR spectroscopy of the rough and flat SiO_2/PDMS films. All samples show high IR absorptance with dips at 9.1, 9.8, and 12 μm wavelengths. The rough samples showed higher absorptance across all wavelengths.

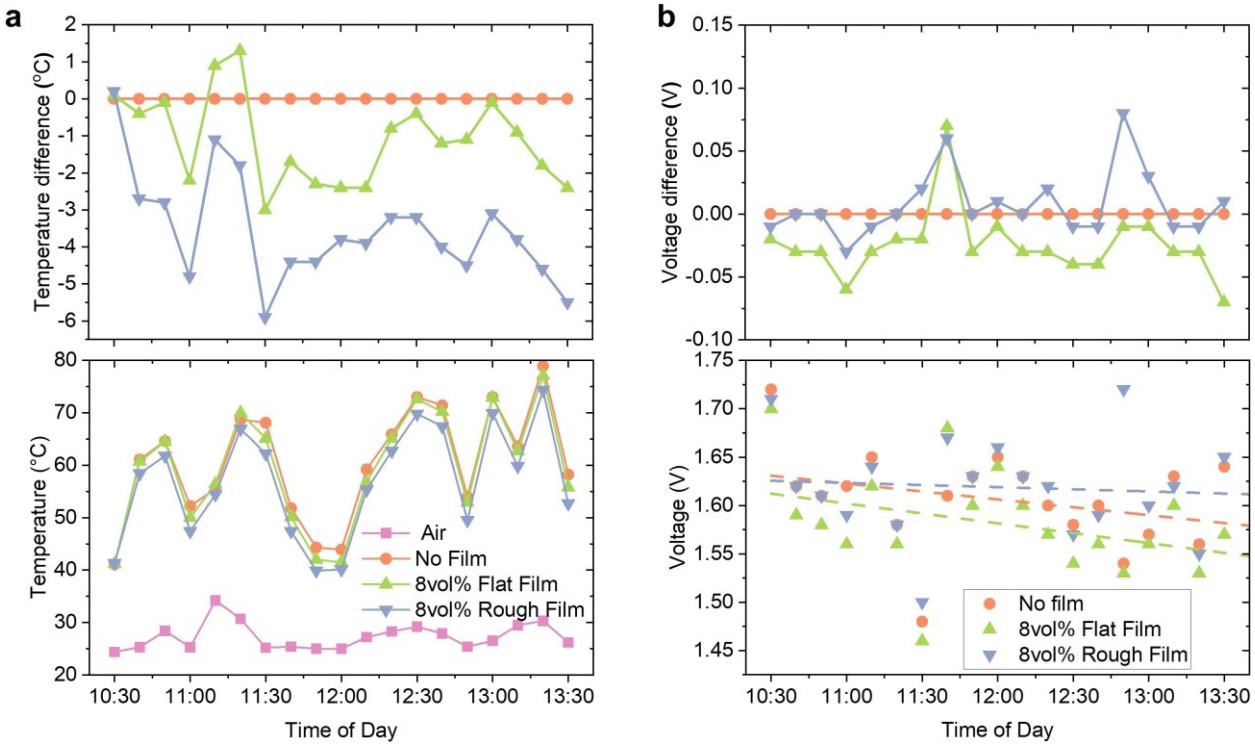

Fig. 5. (a) The temperature difference between the 8vol% SiO_2 films and control (top) as well as the measured temperature (bottom) are shown over the course of the outdoor test. The temperature of the rough film was consistently lower than the control by 3.5°C on average. (b) The voltage difference between the 8vol% SiO_2 films and control (top) as well as the voltage output from each panel (bottom) are shown over the course of the experiment. The voltage difference between each sample is very small showing the film has no negative impact on power generation.

90°C to 29.4°C with sunset being at 7:42 P.M. in the Raleigh area.

The average temperature difference between the solar panels with 8 volume percent SiO_2/PDMS films and the control with no film was 1.1°C and 3.5°C for the flat and rough samples respectively and is shown in Fig. 5 (a). Additionally, the films do not impact the solar panels ability to generate power. The voltage difference between the solar panels with 8 volume percent films and control was 0.04 volts on average and is shown in Fig. 5 (b).

The average temperature difference between the solar panels with 10 volume percent SiO_2/PDMS films and the control was 2.1°C and 3.3°C for the flat and rough films respectively and is shown in Fig. 6 (a). However, it is notable that the 10 volume percent films show a decrease in temperature difference as the experiment progresses. This is likely because the 10 volume percent films were tested late in the day. As the sun began to set, the films were exposed to less direct sunlight and lost performance. When only the first half of the 10 volume percent experiment is considered, the flat and rough films show a 2.9°C and 4.7°C temperature difference below the control respectively. The 10 volume percent films did not impact the power generation of the solar panels and the voltage data is shown in Fig. 6 (b). The rough 10 volume percent film had a voltage that was as much as 0.03 volts higher than the 10 volume percent flat film. It is possible that this could be due to the rough film acting as an anti-reflective coating for the solar cell [30, 31, 32].

For both volume percents, the rough samples consistently provided a greater temperature difference below the control. This is due to the increased surface area of the rough films which led to greater amounts of radiation being emitted. Furthermore, increased amounts of SiO_2 nanoparticles also contributed to greater temperature differences. Furthermore, it can be expected that at higher temperatures and lower humidity, such as desert or space environments, passive cooling of our films given their parameters could show a stronger impact and positively affect the voltage output [33].

4. Conclusion

A composite film was developed that enables the passive cooling of solar panels while having minimal impacts on their power generating efficiency. This film was manufactured utilizing a novel roll coating process. An SiO_2/PDMS nanocomposite polymer-film was produced which included a rough surface topography in order to enhance emittance in mid-IR. The topography of these films was generated by exploiting ribbing instabilities in roll coated polymers. The positive pressure gradient created as a fluid passes between two rollers causes a random micro structure to be formed. Furthermore, the samples

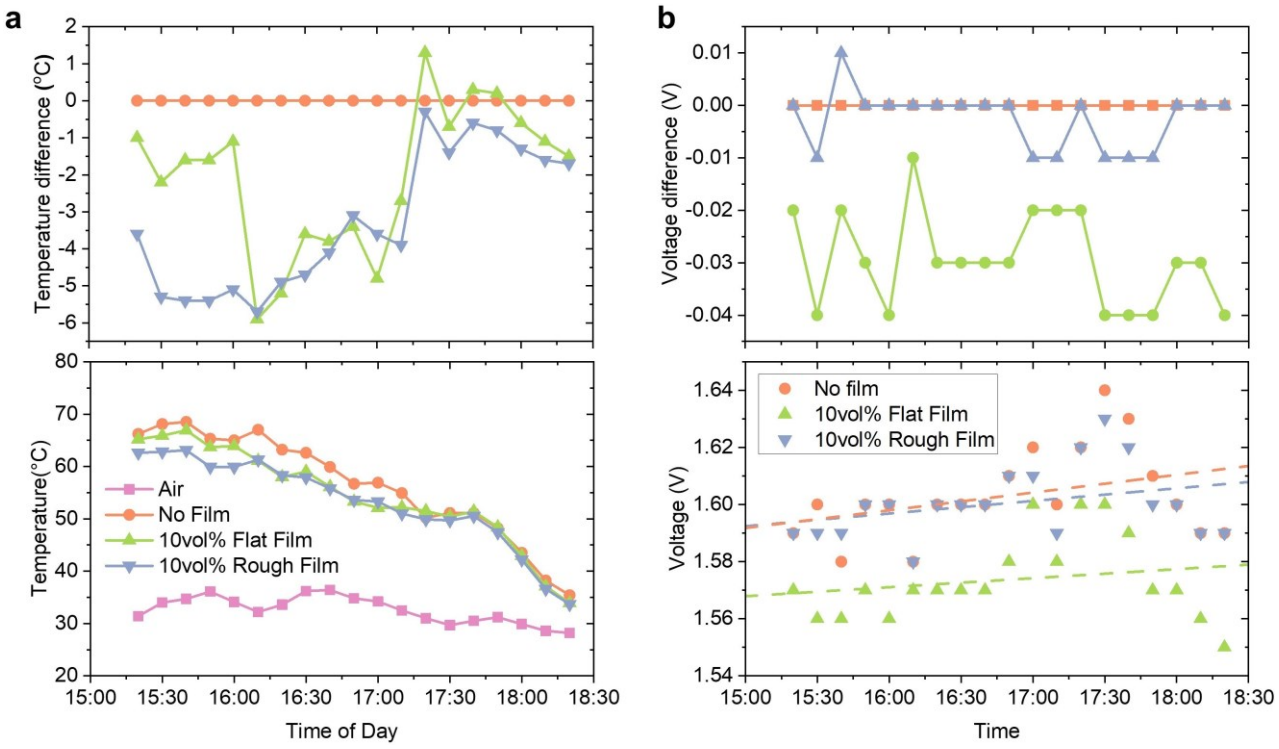

Fig. 6. (a) The temperature difference between the 10vol% SiO_2 films and control (top) as well as the measured temperature (bottom) are shown over the course of the outdoor test. The temperature of the rough film was significantly lower than the control by 4.7°C for the first half of the test. The difference in temperature of the films decreased as the sun set and they were exposed to less direct sunlight. (b) The voltage difference between the 10vol% SiO_2 films and control (top) as well as the voltage output from each panel (bottom) are shown over the course of the experiment. The voltage of the rough film was very similar to that of the panel with no film.

with rough surface topography were shown to have high water contact angles promoting anti-fouling merits.

Optically, the films were shown to have high transmission in the visible spectrum while having increased emission in mid-IR. During outdoor testing, it was found that this film can decrease surface temperature of a solar panel by 3.5°C on average while having minimal impact upon the electrical efficiency of the solar cell. The critical values of our manufactured composite films can be found in Table 1.

The manufacturing methods used to create these films are cost effective, scalable, and fast. On a small scale, several films can be made in the span of a few hours and the process could be easily scaled by increasing the size of the manufacturing machine. This solves several problems that are created by traditional manufacturing techniques such as compression molding and photolithography. Furthermore, the roll coated films perform similarly to films made in previous studies which use other more costly manufacturing processes.

Table 1. Critical results for the 8 and 10 vol% films.

	8 Vol% Film	10 Vol% Film
Rough Film WCA	134°	136°
Peak Density (Avg)	4.71 mm^{-2}	6.162 mm^{-2}
Peak Height (Avg)	456 µm	342 µm
Voltage Difference (Avg)	0.013 V	0.003 V
Temperature Difference (Avg)	3.5°C	3.3°C
Temperature Difference (Max)	5.5°C	5.7°C

Acknowledgements

This research is based upon work supported by the start-up fund by Pratt School of Engineering, Duke University (P. Hsu), NCSU Faculty Research and Professional Development award (J. Ryu), and National Science Foundation under grant No. 2031558 (J. Ryu) and grant No. CMMI-2134664 (Y. Zhu). Part of this work was performed at the Analytical Instrumentation Facility (AIF) at North Carolina State University, which is supported by the State of North Carolina and the National Science Foundation (award number ECCS-2025064). We also thank Dr. Benjamin J. Wiley for the help of the UV-Vis measurement.

References

[1] Allison M. Borchers, Irene Xiarchos, Jayson Beckman, Determinants of wind and solar energy system adoption by U.S. farms: A multilevel modeling approach, Energy Policy, Volume 69, 2014, Pages 106-115, ISSN 0301-4215, https://doi.org/10.1016/j.enpol.2014.02.014.

[2] Solar energy. IRENA. (n.d.)., from https://www.irena.org/Energy-Transition/Technology/Solar-energy

[3] Shuai Li, Zhihua Zhou, Junwei Liu, Ji Zhang, Huajie Tang, Zhuofen Zhang, Yanling Na, Chongxu Jiang, Research on indirect cooling for photovoltaic panels based on radiative cooling, Renewable Energy, Volume 198, 2022, Pages 947-959, ISSN 0960-1481, https://doi.org/10.1016/j.renene.2022.08.020.
[4] M.M. Rahman, M. Hasanuzzaman, N.A. Rahim Effects of various parameters on PV-module power and efficiency Energy Convers. Manag., 103 (2015), pp. 348-358
[5] Bin Zhao, Mingke Hu, Xianze Ao, Qingdong Xuan, Gang Pei, Spectrally selective approaches for passive cooling of solar cells: A review, Applied Energy, Volume 262, 2020, 114548, ISSN 0306-2619, https://doi.org/10.1016/j.apenergy.2020.114548.
[6] S. Niz˘etic´, F. Grubis˘ic´- C˘abo, I. Marinic´-Kragic´, A.M. Papadopoulos Experimental and numerical investigation of a backside convective cooling mechanism on photovoltaic panels
[7] Lina Cui, Canyi Huang, Hong Xia, Yiping Qiu, Qing-Qing Ni, Transparent passive-cooling composite films for indoor and outdoor spaces, Composites Communications, Volume 24, 2021, 100611, ISSN 2452-2139, https://doi.org/10.1016/j.coco.2020.100611.
[8] Hua Bao, Chen Yan, Boxiang Wang, Xing Fang, C.Y. Zhao, Xiulin Ruan, Double-layer nanoparticle-based coatings for efficient terrestrial radiative cooling, Solar Energy Materials and Solar Cells, Volume 168, 2017, Pages 78-84, ISSN 0927-0248, https://doi.org/10.1016/j.solmat.2017.04.020.
[9] S. Fan, A. Raman Metamaterials for radiative sky cooling Natl. Sci. Rev., 5 (2018), pp. 132-133, 10.1093/nsr/nwy012
[10] X. Yin, R. Yang, G. Tan, S. Fan Terrestrial radiative cooling: using the cold universe as a renewable and sustainable energy source Science, 370 (2020), pp. 786-791, 10.1126/science.abb0971 80-.
[11] C. Lin, Y. Li, C. Chi, Y.S. Kwon, J. Huang, Z. Wu, J. Zheng, G. Liu, C.Y. Tso, C.Y.H. Chao, B. Huang A solution-processed inorganic emitter with high spectral selectivity for efficient subambient radiative cooling in hot humid climates Adv. Mater. (2022), Article 2109350, 10.1002/adma.202109350 2109350
[12] X. Ao, B. Li, B. Zhao, M. Hu, H. Ren, H. Yang, J. Liu, J. Cao, J. Feng, Y. Yang, Z. Qi, L. Li, C. Zou, G. Pei Self-adaptive integration of photothermal and radiative cooling for continuous energy harvesting from the sun and outer space Proc. Natl. Acad. Sci. USA, 119 (2022), pp. 1-7, 10.1073/pnas.2120557119
[13] Linshuang Long, Yue Yang, Liping Wang, Simultaneously enhanced solar absorption and radiative cooling with thin silica micrograting coatings for silicon solar cells, Solar Energy Materials and Solar Cells, Volume 197, 2019, Pages 19-24, ISSN 0927-0248, https://doi.org/10.1016/j.solmat.2019.04.006.
[14] Jaafar, J., Siregar, J.P., Tezara, C. et al. A review of important considerations in the compression molding process of short natural fiber composites. Int J Adv Manuf Technol 105, 3437–3450 (2019). https://doi.org/10.1007/s00170-019-04466-8
[15] G. A. Zevallos, M. S. Carvalho, M. Pasquali, J. Non-Newtonian Fluid Mech. 2005, 130, 96.
[16] E. Szczurek, et al. (2009) J. Mater. Process. Technol. 209, 3187.
[17] A. J. Babchin, et al. (1981) Adv. Colloid Interface Sci. 14, 251.
[18] R. J. Fields, M. F. Ashby, Philos. Mag. 1976, 33, 33.
[19] A. M. Grillet, A. G. Lee, E. S. G. Shaqfeh, J. Fluid Mech. 1999, 399, 49.
[20] Md Didarul Islam, Himendra Perera, Benjamin Black, Matthew Phillips, Muh-Jang Chen, Greyson Hodges, Allyce Jackman, Yuxuan Liu, Chang-Jin Kim, Mohammed Zikry, Saad Khan, Yong Zhu, Mark Pankow, and Jong Eun Ryu, Template-Free Scalable Fabrication of Linearly Periodic Microstructures by Controlling Ribbing Defects Phenomenon in Forward Roll Coating for Multifunctional Applications, Advanced Materials Interfaces, 2022, DOI: 10.1002/admi.202201237
[21] Prajzler, V., Nekvindova, P., Spirkova, J. et al. The evaluation of the refractive indices of bulk and thick polydimethylsiloxane and polydimethyldiphenylsiloxane elastomers by the prism coupling technique. J Mater Sci: Mater Electron 28, 7951–7961 (2017). https://doi.org/10.1007/s10854-017-6498-1
[22] H. Zhang, et al. (2020) Proc. Natl. Acad. Sci. U. S. A. 117, 14657.
[23] Y. Zhai, et al. (2017) Science (80-.). 355, 1062.
[24] J. Kischkat, S. Peters, B. Gruska, M. Semtsiv, M. Chashnikova, M. Klinkmu¨ller, O. Fedosenko, S. Machulik, A. Aleksandrova, G. Monastyrskyi, Y. Flores, and W. T. Masselink. Mid-infrared optical properties of thin films of aluminum oxide, titanium dioxide, silicon dioxide, aluminum nitride, and silicon nitride, Appl. Opt. 51, 6789-6798 (2012)
[25] Mao-Qin Lei, Yu-Fan Hu, Ying-Nan Song, Yue Li, Yong Deng, Kai Liu, Li Xie, Jian-Hua Tang, Dong-Lin Han, Jun Lei, Zhong Ming Li, Transparent radiative cooling films containing poly(methylmethacrylate), silica, and silver, Optical Materials, Volume 122, Part B, 2021, 111651, ISSN 0925-3467 (https://www.sciencedirect.com/science/article/pii/S092534672100851X)
[26] Karthik Raman, T.R Srinivasa Murthy, G.M. Hegde, Fabrication of Refractive Index Tunable Polydimethylsiloxane Photonic Crystal for Biosensor Application, Physics Procedia, Volume 19, Pages 146-151, ISSN 1875-3892, https://doi.org/10.1016/j.phpro.2011.06.139.
[27] G. Polizos, G.G. Jang, D.B. Smith, F.A. List, M.G. Lassiter, J. Park, P.G. Datskos, Transparent superhydrophobic surfaces using a spray coating process, Solar Energy Materials and Solar Cells, Volume 176, 2018, Pages 405-410, ISSN 0927-0248, https://doi.org/10.1016/j.solmat.2017.10.029.
[28] Yun-Yun Quan, Li-Zhi Zhang, Experimental investigation of the anti-dust effect of transparent hydrophobic coatings applied for solar cell covering glass, Solar Energy Materials and Solar Cells, Volume 160, 2017, Pages 382-389, ISSN 0927-0248, https://doi.org/10.1016/j.solmat.2016.10.043.
[29] Rima J. Isaifan, Daniel Johnson, Luis Ackermann, Benjamin Figgis, Mohammed Ayoub, Evaluation of the adhesion forces between dust particles and photovoltaic module surfaces, Solar Energy Materials and Solar Cells, Volume 191, 2019, Pages 413-421, ISSN 0927-0248, https://doi.org/10.1016/j.solmat.2018.11.031.
[30] Longqiang Ye, Yulu Zhang, Xinxiang Zhang, Teng Hu, Rui Ji, Bin Ding, Bo Jiang, Sol–gel preparation of SiO2/TiO2/SiO2–TiO2 broadband antireflective coating for solar cell cover glass, Solar Energy Materials and Solar Cells, Volume 111, 2013, Pages 160-164, ISSN 0927-0248, https://doi.org/10.1016/j.solmat.2012.12.037.
[31] Kanmaz, I., Mandong, A. and Uzum, A. Solution-based hafnium oxide thin films as potential antireflection coating for silicon solar cells. J Mater Sci: Mater Electron 31, 21279–21287 (2020). https://doi.org/10.1007/s10854-020-04640-9
[32] Lu Y, Chen Z, Ai L, Zhang X, Zhang J, Li J, et al. A universal route to realize radiative cooling and light management in photovoltaic modules. Sol RRL 2017;1:1700084.
[33] Li, X., Sun, B., Sui, C., Nandi, A., Fang, H., Peng, Y., Tan, G. and Hsu, P.C., 2020. Integration of daytime radiative cooling and solar heating for year-round energy saving in buildings. Nature communications, 11(1), p.6101